

A STUDY ON FIELD ERROR OF BULK HTSC STAGGERED ARRAY UNDULATOR ORIGINATED FROM VARIATION OF CRITICAL CURRENT DENSITY OF BULK HTSCS*

T. Kii[#], R. Kinjo, M. A. Bakr, Y.W. Choi, K. Yoshida, S. Ueda, M. Takasaki, K. Ishida, N. Kimura, T. Sonobe, K. Masuda, H. Ohgaki, Institute of Advanced Energy, Kyoto, Japan.

Abstract

The bulk high-temperature superconductor staggered array undulator (bulk HTSC SAU) has potential to generate strong periodic magnetic field in short period and to control K value without mechanical gap control structure [1]. However, availability of the bulk HTSC magnets having matched performance of critical current density is a problem to be solved. In this study, we have numerically estimated influence of variation of critical current density upon field error using a loop current model based on the Bean model for a type-II superconductor. It was numerically found that the field error was naturally suppressed.

INTRODUCTION

In order to realize strong periodic magnetic field in short period, we proposed the bulk high-temperature superconductor staggered array undulator (bulk HTSC SAU) [2, 3]. The bulk HTSC SAU consists of stacked bulk superconductor magnets inserted in a solenoid magnet as shown in fig.1.

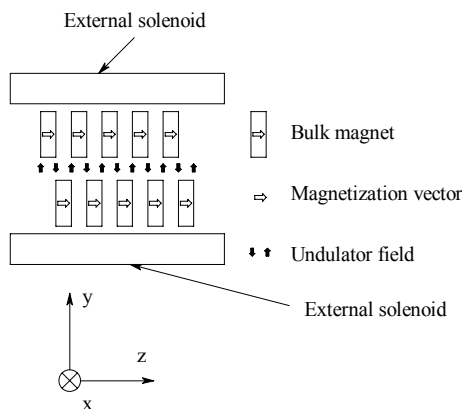


Figure 1: Schematic drawing for principle of the bulk HTSC SAU. Stacked bulk HTSCs are magnetized by an external solenoid. The transverse magnetic field (B_y) is produced by these bulk SC magnets.

The bulk HTSC SAU works as follows. The stacked array is cooled down below the critical temperature in the presence of magnetic field B_{start} . Next, the solenoid field strength is changed to B_{end} . Then, superconducting loop current appears from outer rim toward to inner part of each bulk HTSCs until the supercurrent compensates for the effect by the field change from B_{start} to B_{end} . As the

results, the transverse field component B_y is generated by the superconducting current loops excited in the each bulk HTSC magnet. Here, it is noted that the superconducting currents is determined by the field difference $\Delta B = |B_{start} - B_{end}|$ which is defined by the solenoid and the magnetic field generated by stacked bulk HTSCs.

The features of the undulator are listed below.

- Undulator field can be generated using single solenoid magnet.
- No mechanical structure is required in controlling undulator field.

In order to prove the principle of the bulk HTSC staggered array undulator and estimate the performance, a prototype undulator consisting of a 11 periods of stacked array, a liquid nitrogen cooled vacuum duct, and a normal conducting solenoid was developed [2]. The schematic drawing of the prototype undulator is shown in fig. 2. Detail of copper pieces and DyBaCuO bulk superconductors is shown in fig. 3. Typical trapped field distribution of bulk HTSCs at 77K is shown in fig 4. The average and standard deviation of maximum trapped field of 22 pieces of bulk superconductor were 0.11 T and 0.017 T respectively.

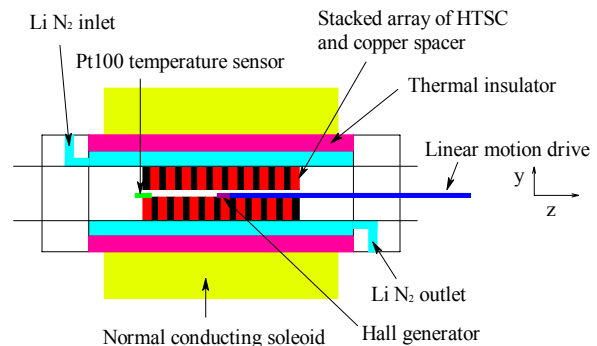


Figure 2: Schematic view of the prototype undulator.

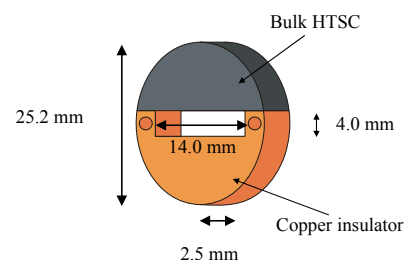


Figure 3: Half period of the stacked array.

*Work supported by Grant-in-Aid for Scientific Research (B) and for JSPS Fellows

[#]kii@iae.kyoto-u.ac.jp

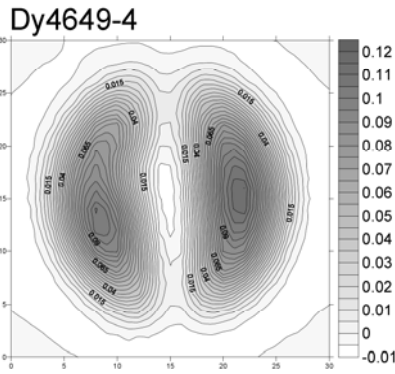


Figure 4: Trapped field distribution at 77K. Magnetic field was measured by using a Hall generator. Distance between the Hall generator and the bulk HTSC was 0.5 mm.

The transverse field distribution along z axis for the field difference of 0.027 T is shown in fig. 5. The undulator field at $z = 0$ was 0.0018 T and standard deviation for central 6 peaks was 3.9 %. As increasing the field difference ΔB , undulator field increases, and the standard deviation also increases as shown in fig. 6. Although the standard deviation for maximum trapped field of each bulk HTSC is 15%, the field flatness is less than 15 % for $\Delta B < 0.09$ T, i.e. field error is suppressed.

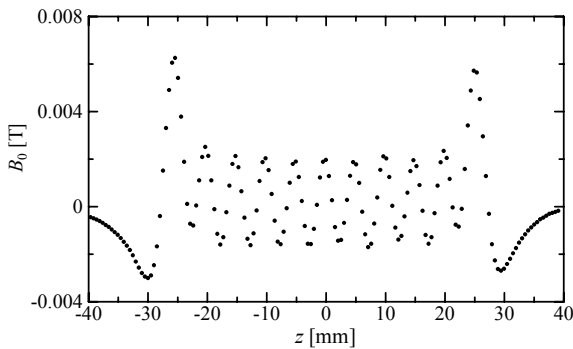


Figure 5: Transverse field distribution at 77K.

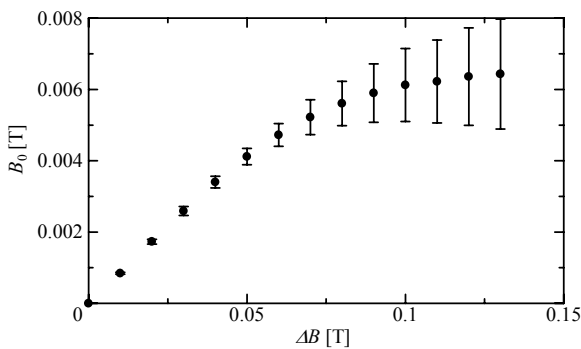


Figure 6: Field strength and standard deviation in central 6 peaks as function of ΔB .

MODEL

In order to investigate origin of the suppression of the field fluctuation and to evaluate the effect of variation of critical current density for bulk HTSCs, we used the numerical calculation code [1] based on the loop current model based on Bean model of type II superconductor [4]. Schematic drawing of the loop current model is shown in fig. 7. Here, D_x , D_y and D_z indicate the size of the bulk HTSC. N_y and N_x indicate the number of total loop in y and z dimension, and n_y indicates the number of supercurrent loop respectively. When the field difference ΔB is applied, supercurrents are induced in the bulk HTSCs from outer rim according to Faraday's law of induction. Current flowing region d_y and current I_c is determined by the critical current density J_c . Here, the penetration ratio of the magnetic field in bulk HTSC Λ_d is defined as $\Lambda_d = d_y/D_y/2$. In the code, the critical current density J_c is field-independent. In order to determine the penetration ratio Λ_d , number of supercurrent loop n_y are iteratively scanned until the magnetic field at the center of each bulk magnet become equal to the field difference ΔB .

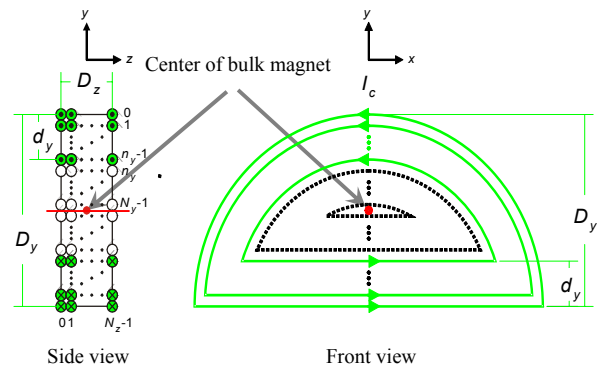


Figure 7: Numerical model of bulk HTSC magnet. The bulk was expressed by $N_y \times N_z$ loops. Green lines indicate the loops in which the supercurrent flows, and black lines indicate the loops without supercurrent. The red point indicates the centre of bulk magnet ($D_y/2, D_z/2$).

The effect of variation of critical current density was evaluated as follows. First, transverse field distribution is calculated with bulk HTSCs having same critical current density J_c . Secondly, critical current density of one bulk HTSC is changed as shown in fig. 8. Thirdly, the number of supercurrent loop n_y is calculated iteratively. Finally, the field strength at the right side of the modified bulk HTSC (red solid circle in fig. 8) is calculated.

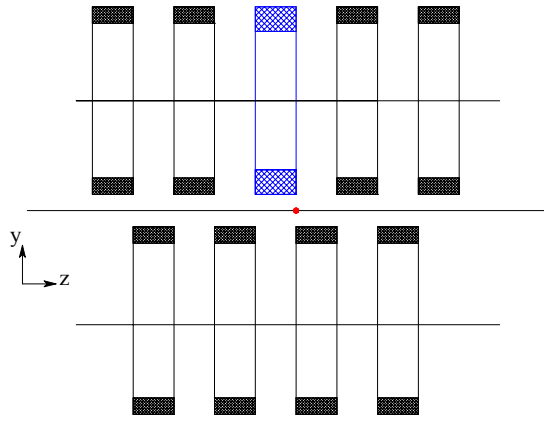


Figure 8: Model to estimate the effect of variation in critical current density. Hatched area indicates the current flowing region. Transverse magnetic field at the red solid circle is compared with changing the critical current density for blue bulk.

RESULTS AND DISCUSSION

Transverse field dependence on critical current density and geometric condition is numerically investigated. Parameters used for calculations are listed in table 1. Typical transverse field distribution is shown in fig. 9.

Penetration Ratio

The penetration ratio of the magnetic field in bulk HTSC λ_d is chosen as about 10 % for standard. Relation between critical current density and number of supercurrent loop n_y is investigated by changing the critical current density of all the bulk HTSC. Results are reproduced by $1/J_c$ law as shown in fig. 10. The relation indicates that the magnetic field on the center of HTSC is proportional to $J_c \times n_y$.

Table 1: Used Parameters for Calculations

Name	Definition	Values
λ_u	Period	5 mm
g	Gap	2 mm, 4 mm
N	Number of period	31
R	Radius of bulk	12.6 mm
D_y	Size of bulk (y)	$R-g/2$
D_z	Size of bulk (z)	$\lambda_u/2$
J_c	Critical current density	133.3 ~ 221.8 A/mm ² (177.45 A/mm ² ± 25 %)
ΔB	Field difference	0.065 T

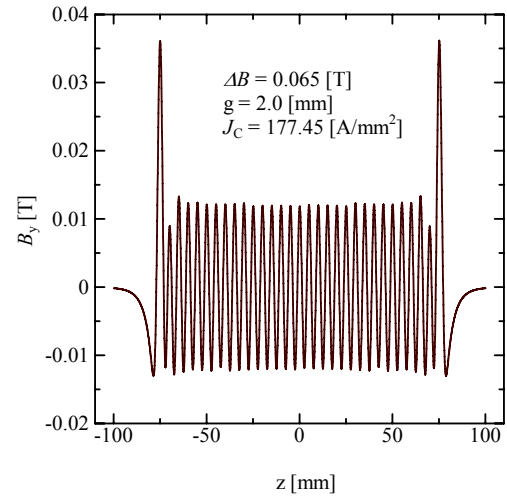


Figure 9: Typical transverse field distribution.

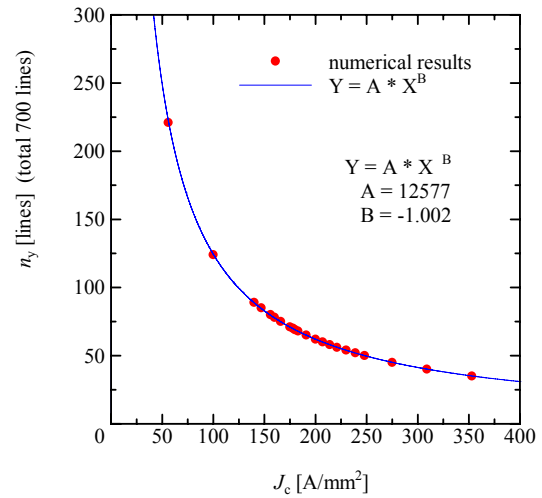


Figure 10: Relationship between the number of supercurrent loop n_y and critical current density J_c .

Field Error Suppression

In order to investigate the field error suppression mechanism, peak field dependence on critical current density of single bulk HTSC is estimated. The critical current density is fixed to 177.45 A/mm² except 32nd bulk. The dependence of transverse magnetic field on critical current density is shown in fig. 11. Though transverse magnetic field increases as increasing the critical current density, the gradient is smaller than 1.0. Suppression ratio is almost 6 for increment of the critical current density.

On the other hand, the suppression ratio for decrement is smaller than that for increment. In addition, the suppression ratio in the case for gap of 4.0 mm is smaller than that of 2.0 mm. In order to survey geometrical effect on the suppression ratio, relation between transverse magnetic field and distance between center of the undulator ($y = 0$) and the inner rim of the current flowing region are evaluated. Results are shown in fig. 12. The transverse field strength linearly decreases as increasing the distance.

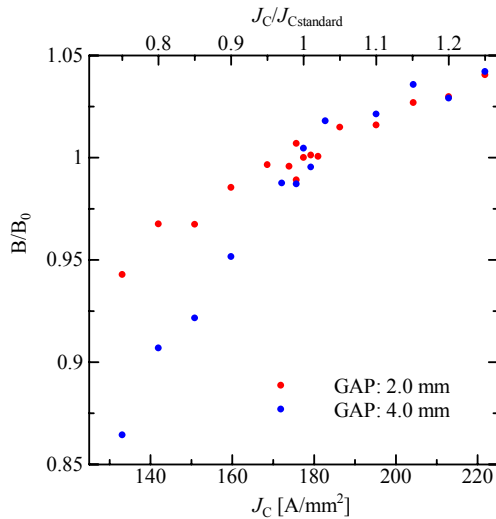


Figure 11: The dependence of transverse magnetic field on critical current density in 32nd bulk HTSC.

CONCLUSION

Field error suppression was observed in bulk HTSC SAU. In order to investigate the mechanism of the suppression of field error, we have studied on field dependence on the critical current density. It was found that current flowing region in the bulk HTSC automatically ranges according to Faraday's law of induction. The automatic ranging successfully suppresses the field error. The suppression ratio is about 6. Consequently, requirement for uniformity of critical current density is moderated.

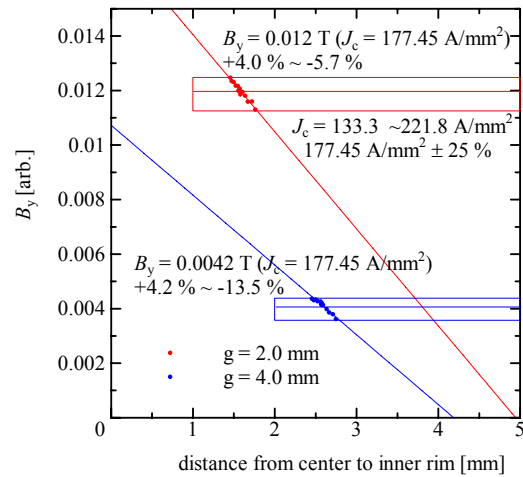


Figure 12: Relation between transverse magnetic field and distance between center of the undulator ($y = 0$) and the inner rim of the current flowing region.

REFERENCES

- [1] R. Kinjo, et al., "NUMERICAL EVALUATION OF BULK HTSC STAGGERED ARRAY UNDULATOR BY BEAN MODEL", Proceedings of FEL 2009, 746 (2010).
- [2] R. Kinjo, et al., "BULK HIGH-TC SUPERCONDUCTOR STAGGERED ARRAY UNDULATOR", Proceedings of FEL 2008, 473 (2009).
- [3] T. Kii, et al., "Proposal of a Bulk HTSC Staggered Array Undulator", AIP Conf. Proc. of SRI 09, 539 (2010).
- [4] C. P. Bean, "Magnetization of High-Field Superconductors", Rev. Mod. Phys. 36, 31 (1964).